Modeling the percentage of solids in bauxite mining tailings using geoprocessing

http://dx.doi.org/10.1590/0370-44672022760079

Mauro de Castro Lima Filho[1,2,5]
https://orcid.org/0000-0002-3279-2706
Patrícia Sousa Silva[1,2,6]
https://orcid.org/0000-0002-0721-6571
Júlio Alencar[1,7]
https://orcid.org/0000-0002-4828-5039
Fabrícia Benda de Oliveira[3,8]
https://orcid.org/0000-0002-4456-0275
Cácio José da Silva[4,9]
https://orcid.org/0009-0004-5467-3937
Leonardo Agripino[2,10]
https://orcid.org/0009-0004-9376-2393

[1]Universidade Federal do Pará – UFPA, Departamento de Engenharia Geotécnica, Belém – Pará – Brasil.

[2]Norsk Hydro Brasil LTDA, Gerência de Geotecnia e Operação de Barragens, Paragominas – Pará - Brasil.

[3]Universidade Federal do Espírito Santo – UFES, Departamento de Geologia, Alegre – Espírito Santo – Brasil.

[4]Norsk Hydro Brasil LTDA, Gerência Técnica, Paragominas – Pará - Brasil.

E-mails: [5]maurogeologia@gmail.com, [6]patricia.sousa.silva@hydro.com, [7]julioalencar.1957@gmail.com, [8]fabriciabenda@gmail.com, [9]cacio.silva@hydro.com, [10]leonardo.agripino@hydro.com

Abstract

Linked to important pillars of the Brazilian economy, studies related to mining and the use of UAVs (unmanned aerial vehicles) have been gaining ground in recent years, especially related to the geotechnics of dams and precision agriculture. However, the interdisciplinarity needed to carry out more robust analyses are still lacking in some areas, which brings up good opportunities to be explored. In this sense, the present study combined products obtained through different activities and methodologies, aiming at a solution that provides predictability to the mining dam management process, specifically linked to modeling and obtaining data on solid content in the tailings, arising from the processing of bauxite, based on geoprocessing. The activities necessary to achieve the sought objectives covered, briefly: 2021 tailings sampling campaign carried out in the Plateau Disposal System (RP1), laboratory analyses (humidity), aerial survey with Unmanned Aerial Vehicle (UAV), geoprocessing for the extraction of luminosity values of images and statistical analysis of dispersion. As a result, it was observed that the increase in the number of drying cracks (highlighted in the images by dark pixels) is directly related to the drying of the waste (increase in the percentage of solids), whose quadratic model presents an excellent relationship between the values of the pixels in the images and percentage of solids from laboratory data, implying a determination coefficient of 91.74%. Furthermore, gains in security, predictability and economy for the processes stand out, when compared to the traditional methods applied, in addition to an excellent potential to be developed in future studies.

Keywords: dams, UAV, drying cracks, predictability.

1. Introduction

Mining dams have the function of adequately containing and storing waste from the ore beneficiation process (ANM, 2022). Compared to agriculture, for example, an activity that occupies large areas and makes constant use of pesticides and fertilizers, mining, in general, has less potential for environmental damage if correctly performed (Luz & Linz, 2018). As for the technical assessments in the context of dams, it is possible to observe a growing tendency towards modernization of the methods and equipment used in the geotechnical monitoring of these structures, obtaining physical-chemical data of the materials and assessments of areas, including diagnosis, mitigation of environmental impacts, optimization processes and maximizing the use of natural resources linked to mining dams. In this way, studies on technology and innovation inherent to mining dams gain investment and prominence. It is possible to highlight the need for monitoring to verify the effectiveness of this disposal, in order to plan, execute and readjusted future plans for the disposal of tailings, aiming at a uniform and optimized distribution of these materials in the reservoir. For this, it is fundamental to understand the drying of the waste in the reservoirs, whose data are conventionally obtained through field collection and laboratory analysis. This drying is strongly influenced by climatic, geological-structural and pedological characteristics, directly influencing the rates of rainfall, evaporation and the permeability of the dam foundation.

Within the scope of understanding the distribution of tailings, volumetric volumes and the like, the use of UAVs is gaining more and more space. Used to capture images of the land surface, followed by adequate processing, they can provide very useful products that are still little explored in the geotechnical environment even though they present good results for the development of advanced techniques and tools, facilitating analyzes in the areas of interest, mainly related to dams (Peters *et al.*, 2020). However, in mining, said equipment and products are normally used for the acquisition of conventional aerial images, preparation of topographic maps, measurement of areas and the like, with their use and development often restricted to the areas of topography, projects and mine planning (including geological modeling, sequencing of mines, etc.), and is still little explored by some areas of said activity.

In this sense, the present article proposes the use of orthophotos to develop more advanced and agile applications, through geoprocessing, aiming at obtaining information that is normally obtained only with methods of sample collection and conventional analysis, as occurs in physical analyses (routinely carried out in the laboratory) to know the solids of the tailings in mining dams.

Occupying an area of around 50,000 km², is the Bauxite Province of Paragominas and its regional context encompasses sediments of eolian and lagoon nature, as well as estuarine-lagunar and fluvio-estuarine, characteristic of coastal environments. Geomorphologically, the region is marked by dissected tabular relief, whose approximate altitudes vary between 400 and less than 100 m, being limited between the Serra de Gurupi and the region of the city of Ipixuna (Kotschoubey *et al.*, 2005). In this geological-geomorphological context, MPSA owns a bauxite mining and processing complex, it also has two Tailings Disposal Systems (TDS): Valley (TDS) and Plateau (SDR2), whose operations began in March 2007, with the provision in the Valley System. In 2017, the Plateau System (RP1), the focus of this study, came into operation, and currently, the arrangement occurs in both systems (Figure 1).

Heterogeneous rock composed mainly of one or more aluminum hydroxides and various mixtures containing silica, iron oxide, titanium, kaolinite and other impurities in smaller quantities, bauxite was discovered in the year 1821, by the scientist Pierre Berthier (1782-1861), in Les Baux, situated in the southern region of France. It is a rock with more than 40% alumina (Bárdossy, 1997; Sampaio *et al.*, 2005).

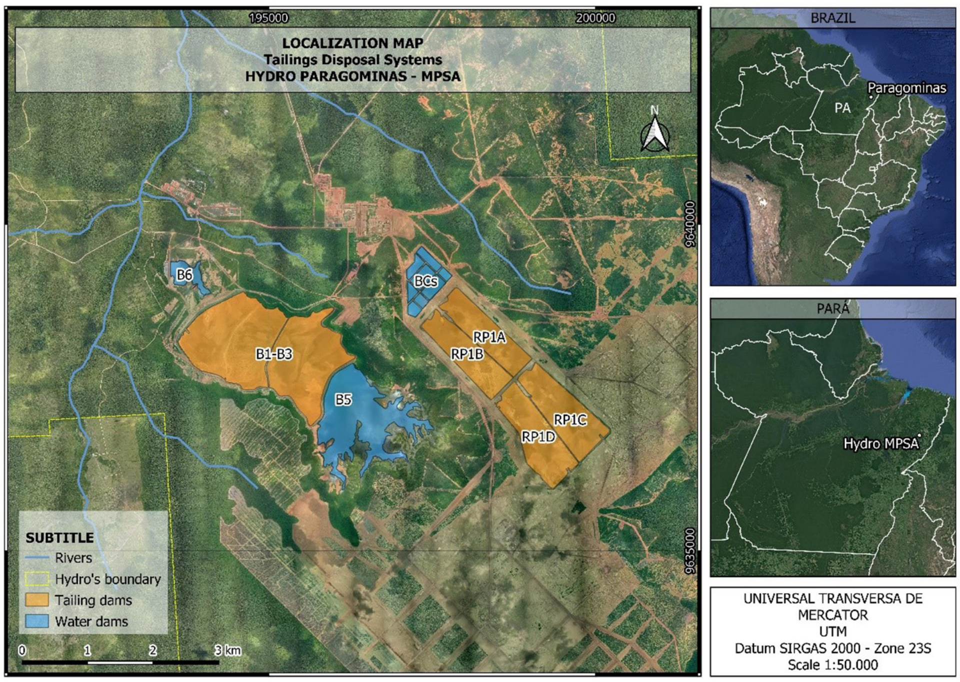

Figure 1 – MPSA-Hydro Tailings Disposal Systems Location Map.

2. Materials and methods

Hydro-MPSA's monthly topographic database for the year 2021 was used, including 12 orthophotos (generated month by month, from January to December) obtained from processing aerial images captured by UAVs. Results of laboratory analyzes (percentage of solids) in the periods of the respective dates of acquisition of aerial images were incorporated into the database for correlation purposes. The following steps were performed: collection of sampling and laboratory data, aerial images, processing, estimates of the percentage of solids and validation of the results obtained. The specific stages of the study will be described below.

To point out that in the MPSA the waste is disposed with a solid content varying between 33% and 35%, then passing through exposure for drying at periods of 30 to 60 days, during the dry season and rainy season, respectively, until it reaches a solid content equal to or greater than 60%, when a new layer is launched, repeating the process cyclically. The tailings from the bauxite beneficiation process are predominantly fines, with a higher fraction passing through at 400 mesh, in which the tailings are disposed of by spigotting, and within the management and planning routine, tests are carried out in accordance with NBR 6457 (ABNT, 1986) and NBR 7217 (ABNT, 1984), for determining moisture, solid content, granulometry and density, for monitoring the evolution of the drying process of the tailings in the dams.

As a way of understanding and managing the solid content of the tailings disposed of in RP1, weekly campaigns are carried out to collect samples of tailings with a specific sampler. The RP1 quadrants have 03 platforms in each of the 04 quadrants and the samples are stored in plastic bags, duly labeled and transported to the laboratory, where they are weighed on high precision scales, dried in an oven and weighed again, obtaining data of dry and wet mass, consequently the respective percentages of solids and moisture contents. Annually, an average of 500 samples are collected, and this routine is carried out twice a week, in the quadrants where waste is being disposed. Field collections and humidity tests are carried out according to Hydro's internal procedure, based on NBR 6457 (ABNT, 1986).

The image acquisition was done using the DJI Phantom 4 RTK model drone and then the processing is performed using the software Agisoft Photoscan, where the workflow makes it possible to obtain point clouds, digital elevation models and the orthophotos to be used to obtain the products.

With the 12 orthophotos from January to December 2021, in a GIS environment, an area with dimensions of 50 m wide by 50 m long was delimited, positioned next to the sampling platforms of the RP1-A quadrant, restricting the areas of existing interest, closer to the collection points of waste samples. As mentioned, the RP1-A has 3 sampling platforms, thus, a total of 36 orthophoto clippings were extracted (1 monthly clipping per platform). Subsequently, to access the quantitative attributes of these images, the values referring to the brightness of the pixels of the images of the referred cutouts were extracted, for points. It is worth mentioning that each of the 3 monthly images generated for analysis contained around 140,000 points, whose attribute tables generated were exported for subsequent analyses.

With the data from the mentioned extraction of pixel luminosity values, their averages were calculated and the percentages of solids in each region were organized, as well as the monthly rainfall, seeking the first understandings about the relative behaviors between the variables. Then, the software used was Minitab (version 20.4) and regression analyses were performed between pixel values (luminosity) and solid content, generating graphs and the like. Thus, it was possible to statistically verify the relationship between the results of solid contents and the luminosity of the pixels in the orthophotos of the tailings.

Finally, aiming at validation, data from March 2022 were used in the model and the results obtained by conventional means (collection and laboratory analysis) were checked, comparatively, even if fed by data from 2021, based on the proposed methodology.

3. Results

With the monitoring and analysis of the laboratory results of the percentage of solids, it was possible to generate a box plot graph and observe the drying process of the waste, its phases and main sub-processes: exudation, evaporation, infiltration, stabilization and formation of drying cracks according to the trend curve (Figure 2). When comparing the average data between the 3 drying phases, it is noted that the 1st and 3rd phases refer to the portions of the curve in which the differences between the sample averages were significant, attesting that there are greater moisture losses, that is, greater variability in the drying period. In the 2nd phase, the differences between the averages were not significant ($p > 0.05$); at this moment there was no significant gain in solid content and loss of moisture.

It should be confirmed that after the stabilization of the 2nd phase a significant gain in solid content occurs due to the three-dimensional development of the referred to drying cracks, again increasing the permeability of the materials and the exposure area, also combined with the high evaporation rates.

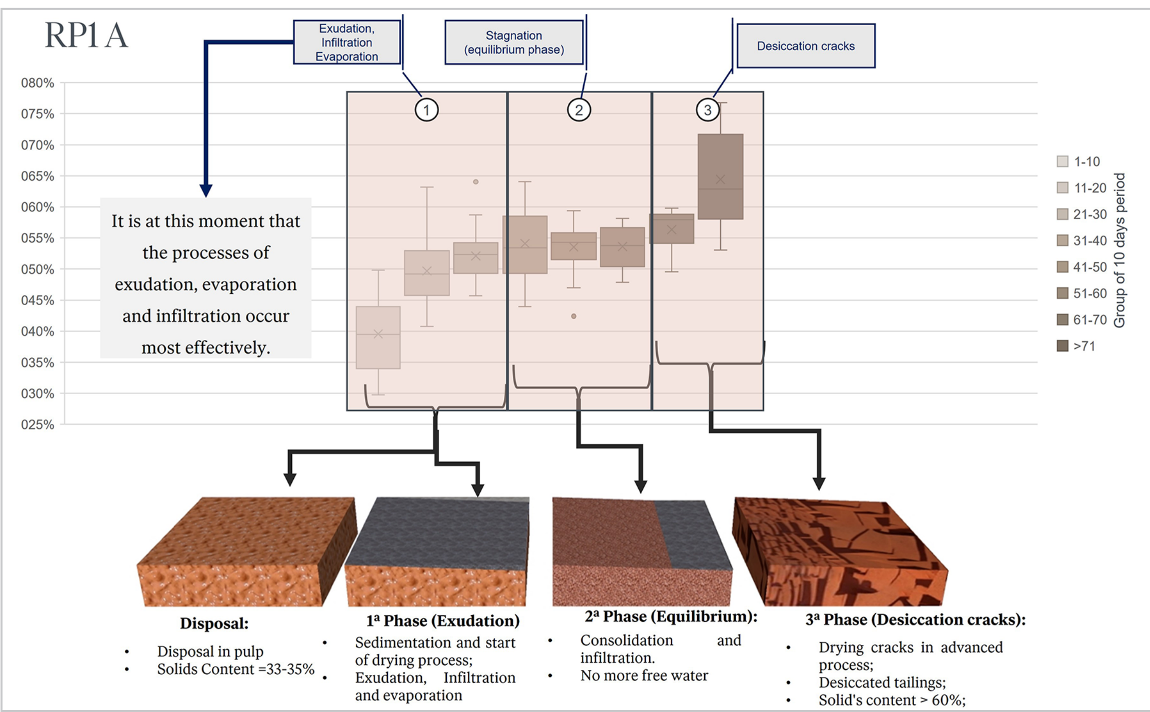

Figure 2 – Percentage of solids in the tailings (y axis) versus days (x axis), highlighting the 3 drying phases after disposal of the tailings.

In addition, as an example of a qualitative result, it is possible to highlight the visual comparison obtained in relation to the raw data of the first semester of 2021 in the RP1-A quadrant, highlighting the change marked by the increase in the concentration of dry cracks, associated with the increase in the percentage of solids on the tailings surface, between January (smoother and clearer due to the tailings surface) and June (more rough and darker due to the increased concentration of contraction cracks) of 2021 (Figure 3).

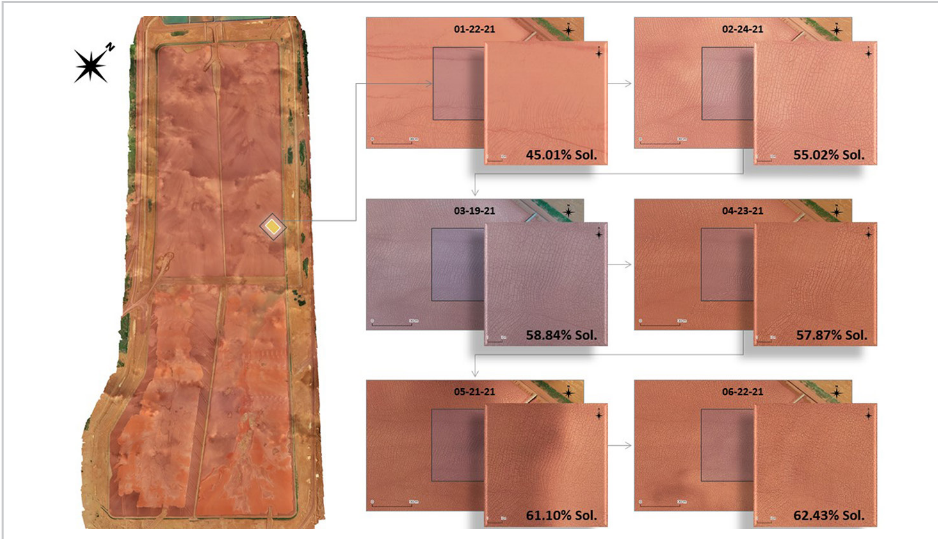

Figure 3 – Variation of solids content in the tailings (quadrant RP1-A) between January 22nd and June 22nd, 2021, on platform 3.

Furthermore, as quantitative results, it was possible to obtain the average luminosity values (through the extraction of these values contained in the pixels of the images) for points whose exportation of the respective tables of attributes and analyses, made possible the first understandings of the relationships between the contents of solids and pixel brightness values (Figure 4).

As expected, it was also possible to verify that the pixels present in the cracks generate lower luminosity values, reaching maximum values of 170, here defined by luminosity units, giving the image darker aspects. On the other hand, the response of the pixels presents on the surface of the waste, generate higher values, surpassing 180 luminosity units, attributing lighter tones to the images (Figure 5).

Based on the statistical analysis, it was possible to obtain the quadratic model, correlating the image variables (pixel luminosity) and the laboratory results (percentage of solids), expressed by the formula used to obtain predictability, as follows:

$$y = 4.091 - 0.03269\,x + 0.000075\,x^2$$

Where: "y" is the percentage of waste solids; and "x" is the brightness value of the pixels.

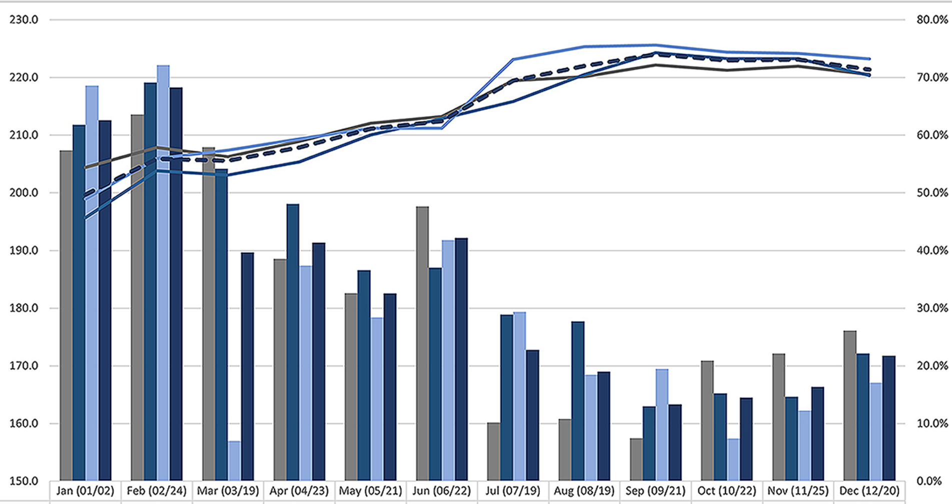

	Jan (01/02)	Feb (02/24)	Mar (03/19)	Apr (04/23)	May (05/21)	Jun (06/22)	Jul (07/19)	Aug (08/19)	Sep (09/21)	Oct (10/22)	Nov (11/25)	Dec (12/20)
Average P1	207.4	213.6	207.9	188.6	182.6	197.6	160.2	160.8	157.5	170.9	172.1	176.1
Average P2	211.8	219.1	204.2	198.1	186.6	187.0	178.9	177.7	163.0	165.2	164.7	172.1
Average P3	218.6	222.2	157.0	187.4	178.4	191.8	179.4	168.5	169.5	157.4	162.2	167.1
Average Pixels	212.6	218.3	189.7	191.4	182.6	192.2	172.8	169.0	163.3	164.5	166.3	171.8
% Solids P1	54.4%	57.9%	56.3%	58.9%	62.1%	63.2%	69.4%	70.2%	72.2%	71.3%	71.9%	70.5%
% Solids P2	45.7%	53.8%	53.1%	55.4%	60.0%	62.8%	65.8%	70.5%	74.3%	73.3%	73.3%	70.3%
% Solids P3	49.0%	56.0%	57.4%	59.3%	61.2%	61.2%	73.1%	75.4%	75.6%	74.4%	74.2%	73.2%
% Average solids	49.7%	55.9%	55.6%	57.9%	61.1%	62.4%	69.5%	72.0%	74.0%	73.0%	73.1%	71.4%

Figure 4 – Luminosity data extracted from the orthophoto and Graph containing pixel luminosity data and percentage of solids measured (laboratory) on the 3 platforms (P1, P2 and P3).

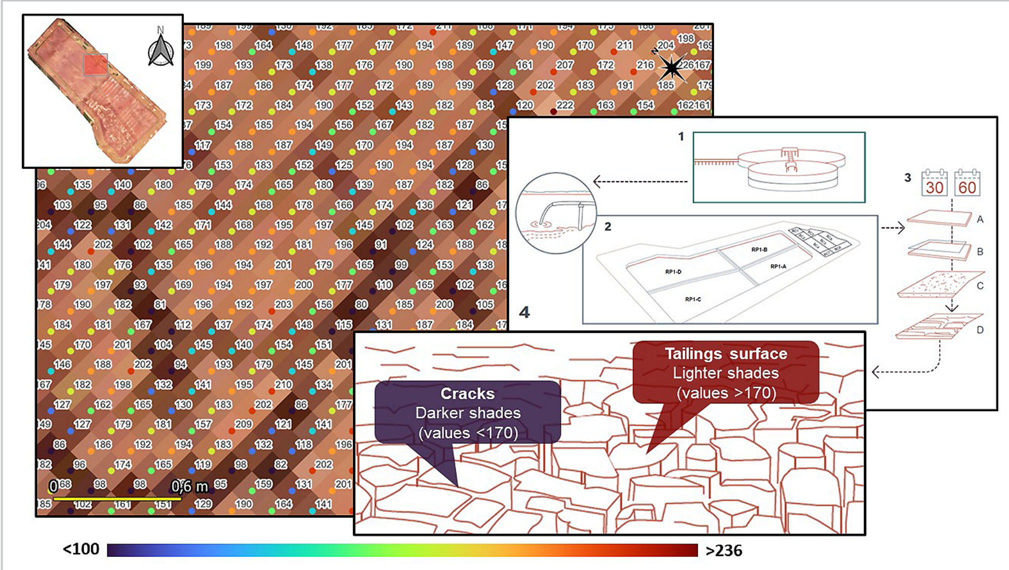

Figure 5 – Pixel luminosity values attest to the significant difference in response between the referred features.

These analyses also allowed us to verify that the value of p (<0.001) indicates that the relationship between the two variables is statistically significant (when $p<0.05$). Furthermore, the value of the coefficient of determination (R^2 = 91.74%) implies a strong correlation between the variables (solid content and pixel luminosity), and the equation for the quadratic model made it possible to obtain a table relating them (Figure 6 and Figure 7).

From the analyses, it was possible to compare the results obtained by conventional means (sampling and laboratory analysis) with the predictability results (pixel luminosity and use of the quadratic model equation) (Figure 8).

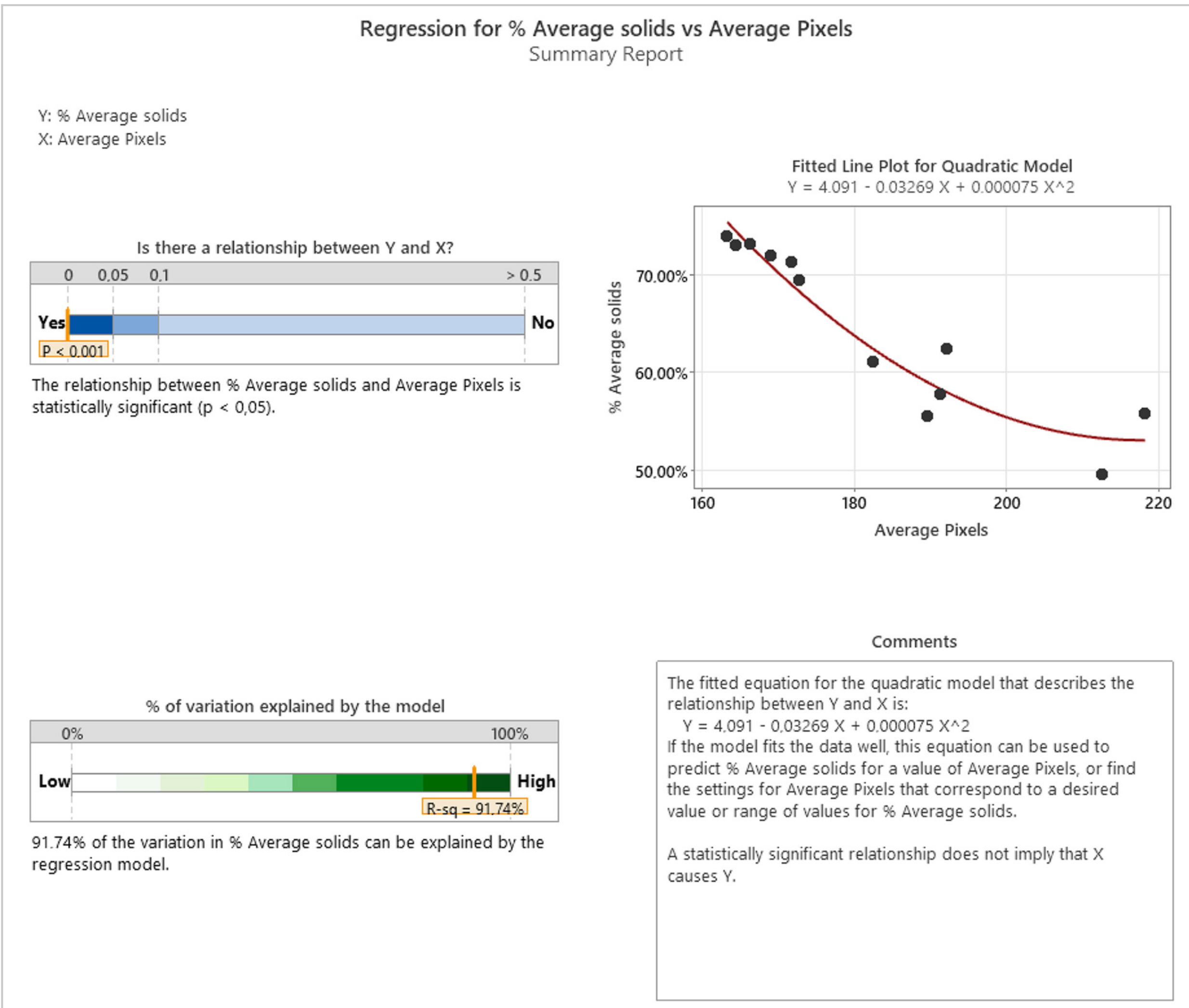

Figure 6 – Summary report generated from regression analyzes with the software Minitab.

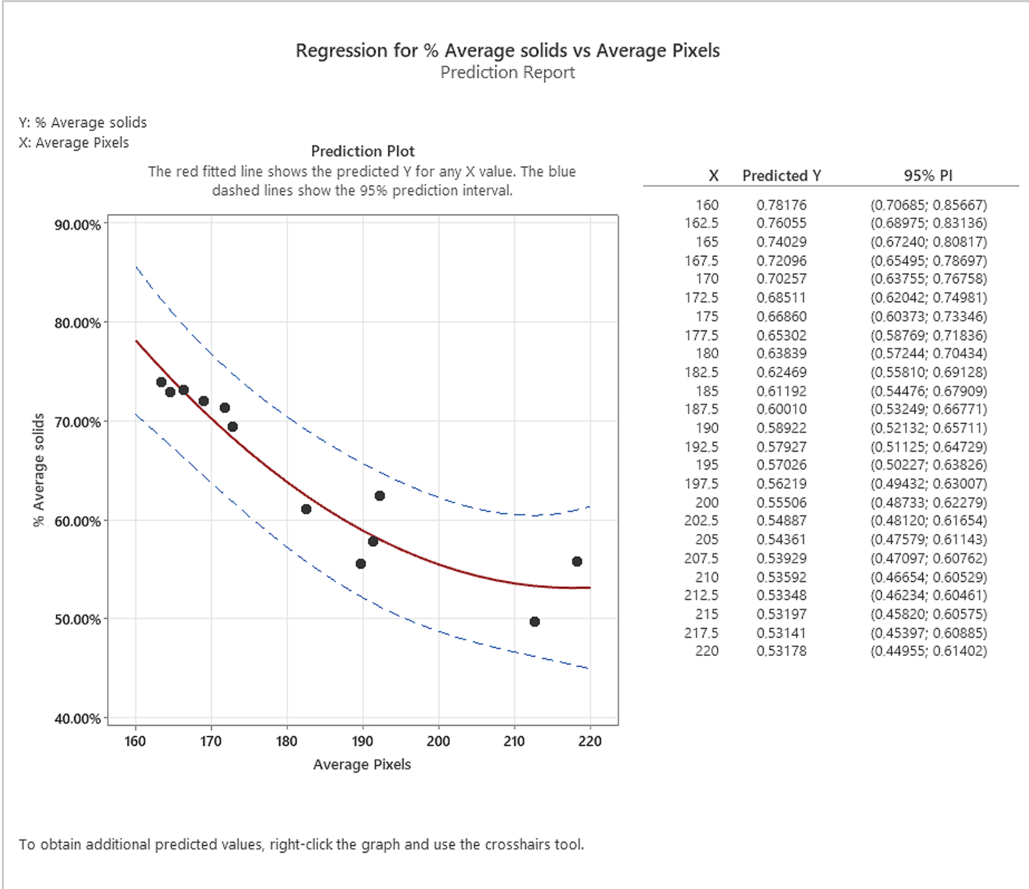

X	Predicted Y	95% PI
160	0.78176	(0.70685; 0.85667)
162.5	0.76055	(0.68975; 0.83136)
165	0.74029	(0.67240; 0.80817)
167.5	0.72096	(0.65495; 0.78697)
170	0.70257	(0.63755; 0.76758)
172.5	0.68511	(0.62042; 0.74981)
175	0.66860	(0.60373; 0.73346)
177.5	0.65302	(0.58769; 0.71836)
180	0.63839	(0.57244; 0.70434)
182.5	0.62469	(0.55810; 0.69128)
185	0.61192	(0.54476; 0.67909)
187.5	0.60010	(0.53249; 0.66771)
190	0.58922	(0.52132; 0.65711)
192.5	0.57927	(0.51125; 0.64729)
195	0.57026	(0.50227; 0.63826)
197.5	0.56219	(0.49432; 0.63007)
200	0.55506	(0.48733; 0.62279)
202.5	0.54887	(0.48120; 0.61654)
205	0.54361	(0.47579; 0.61143)
207.5	0.53929	(0.47097; 0.60762)
210	0.53592	(0.46654; 0.60529)
212.5	0.53348	(0.46234; 0.60461)
215	0.53197	(0.45820; 0.60575)
217.5	0.53141	(0.45397; 0.60885)
220	0.53178	(0.44955; 0.61402)

Figure 7 – Prediction report generated from regression analyzes with the software Minitab.

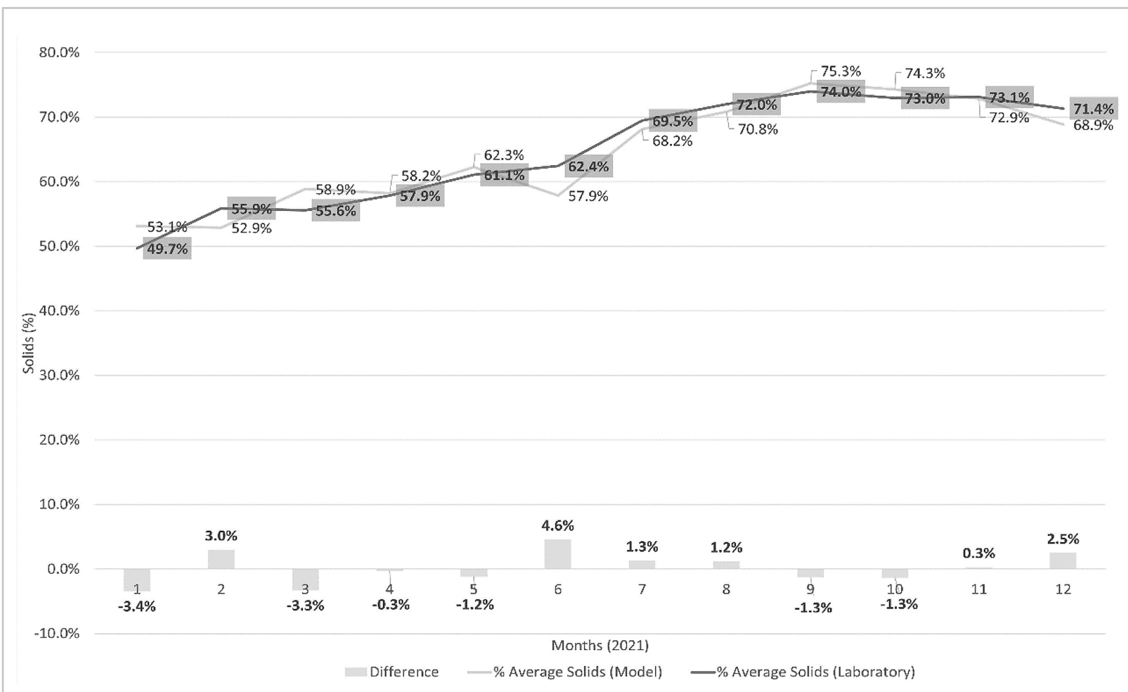

Figure 8 – Comparison between the conventional solids contents and those obtained through the predictability formula.

The average results for the year 2021 indicated a maximum difference of 4.6% between laboratory data and the predictability model.

As a way of validating the model, luminosity values were also extracted from the pixels in the region of the 3 platforms (P1, P2 and P3), using the orthophoto generated on March 25, 2022, using the referred to methodology (Figure 9).

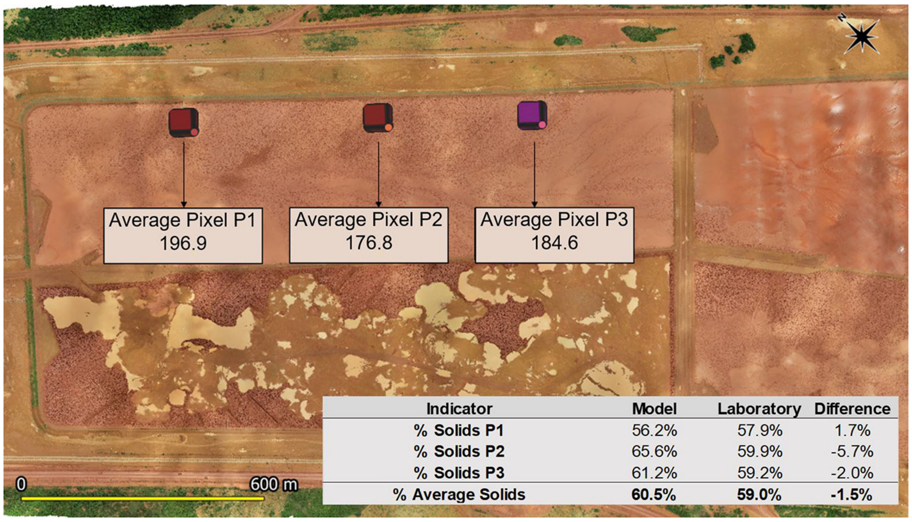

Figure 9 – Luminosity data extracted from the orthophoto of 03/25/2022, highlighting the RP1-A.

The comparative results between the two methods (laboratory versus model) can be seen in Table 1.

Table 1 – Comparison between the results calculated from the predictability model equation and the samples and laboratory analyzes of 03/25/2022.

Indicator	Model	Laboratory	Difference
% Solids P1	56.2	57.9	1.7
% Solids P2	65.6	59.9	-5.7
% Solids P3	61.2	59.2	-2.0
Average % Solids	**60.5**	**59.0**	**-1.5**

It is possible to note that, even considering that the model inputs were from the year 2021, the equation of the generated model showed a maximum variation of 5.7% on platform 2 and in the final average, only 1.5%, when tested with pixel luminosity data from 2022.

4. Discussion

In a brief comparison with other studies, through operations with images, Santos *et al.* (2016) related the perceptible characteristics in the soil to moisture content, obtaining good evidence that the methodology is promising for predictability purposes. Liu *et al.* (2022) also used digital image processing to predict soil moisture content, pointing out that the luminosity parameters extracted from the images, associated with statistical methods of linear regression, generate good results. Evaluating aerial images, it is also possible to observe the most frequent features, shades, etc. And the quantification of these features in the images is feasible through the extraction of the referred to luminosity values, as proposed by Wang & Shi (2006).

As for the present work, at the end of the tailings release, it is possible to infer two trivial initial phases, starting with sedimentation and partial separation between the solid and liquid phases, where there is the greatest advance in the drying process, especially of the supernatant water. This higher initial loss can be justified by the high permeability of the geological-structural units of the Plateau System foundation, combined with the high regional evaporation rates, occurring mainly in the first layers more effectively, due to direct contact with the foundation. Then, there is a stabilization phase, marked by the consolidation and beginning of the development of the three-dimensional mosaic formed by cracks of dryness observed by Pedrosa (2012) (Figure 10).

However, despite not being so obvious, observing and analyzing the dispersion and trend of the data it was also possible to highlight a second significant gain in drying punctuated as a 3rd phase, marked by the three-dimensional evolution of the cracks, consequently greater exposure of the materials in specific area terms.

Figure 10 – Generation of the dry cracks mosaic. Source: Pedrosa (2012).

In this way, it is possible to point out that the development of drying cracks also favors penetrability in the underlying waste and connection, albeit incipient, with the substrate, the foundation, which is significantly permeable. The increase in the exposure area (specific area) also allows for greater effectiveness of the evaporation process. Furthermore, the relationship between the increase in the concentration of cracks implies the "darkening" of the orthophotos; that is, with the advancement of the drying of the tailings, there is an increase in the number of dark pixels, whose luminosity values are obviously lower than those disposed on the surface of the tailings.

These understandings obtained through systemic and interdisciplinary analysis (geotechnics, geoprocessing, and statistics) are the core of this study and are fundamental for understanding the results.

5. Conclusions

Given the above, it was possible to observe that the laboratory results provide essential data for understanding the behavior during the drying of the tailings in RP1. The evolution curves of this drying make clear the different stages of this process, from its disposition to drying and intensification of the quantity of drying cracks.

By correlating empirical observations and laboratory data, it was possible to visualize the increase in the percentage of solids in the waste, obtained over the drying time, attributing the increase in the number of cracks to the reduction in the average of the luminosity values in the orthophotos, whose relationship was statistically proven.

Therefore, the interdisciplinary methodology, encompassing geoprocessing, geotechnics and statistics, is applicable and deserves attention for future work. It is also recommended to apply the method with the use of special sensors, such as thermals, LiDAR (Laser Detection and Ranging), among others applicable to the topics discussed throughout the article.

Finally, with the equation obtained, expressed in the results, as well as the robust database of laboratory results and aerial survey routine, it is possible to reassess the need for the current weekly sampling volume practiced in the company. In this way, the application of the proposed method proves to be viable for monitoring the drying process of the waste (from 35% to 60% of solids), being recommended to prove the target percentage (60%) and the release of the layers maintained by the conventional (laboratory) method.

Considering the aforementioned statistical evidence, the use of the interdisciplinary methodology proved to be promising, where it was possible to attest to the feasibility of obtaining the predictability of the percentage of solids in the waste from the bauxite beneficiation process, whose reduction in the sampling routine can generate labor savings of work and materials, intended for sampling and use in the company's laboratory, just better exploring the data and resources already existing in the company.

References

AGÊNCIA NACIONAL DE MINERAÇÃO - ANM (Brasil). ***Resolução ANM n. 95, de 7 de fevereiro de 2022.*** Consolida os atos normativos que dispõem sobre segurança de barragens de mineração. Diário Oficial da União, Edição 33, 49. Disponível em : https://www.in.gov.br/en/web/dou/-/resolucao-n-95-de-7-de-fevereiro-de-2022-380760962. Acesso em: 22 de Setembro de 2022.

BARDOSSY, GYORGY. Berthier, les Baux et l'histoire de la bauxite. ***Comptes Rendus de l'Académie des Sciences - Series II A - Earth and Planetary Science,*** v. 324, n. 12, p. 1031-1040, 1997.

KOTSCHOUBEY, B.; CALAF, J. M. C.; LOBATO, A. C. C.; LEITE, A. S.; AZEVEDO, C. H. D. Caracterização e gênese dos depósitos de bauxita da província bauxitífera de Paragominas, Nordeste da bacia do Grajaú, Nordeste do Pará/ Oeste do Maranhão. ***Caracterização de depósitos minerais em distritos mineiros da Amazônia,*** p. 687-782. 2005.

LIU, G.; TIAN, S.; MO, Y.; CHEN, R.; ZHAO, Q. On the acquisition of high-quality digital images and extraction of effective color information for soil water content testing. ***Sensors,*** v. 22, n. 9, 3130, 2022.

MORRIS K., Thomas (1908-1992). ***ModernLogic,*** v. 3, nº. 2, p. 156-158, 1993.

ASSOCIAÇÃO BRASILEIRA DE NORMAS TÉCNICAS - ABNT. ***NBR 7181*****:** solo - análise granulométrica. Rio de Janeiro, 1984.

ASSOCIAÇÃO BRASILEIRA DE NORMAS TÉCNICAS - ABNT. ***NBR 6457*****:** amostras de solo - preparação para ensaios de compactação e ensaios de caracterização. Rio de Janeiro, 1986.

PEDROSA, G. J. ***Modelação física da disposição de rejeitos de bauxita por meio de diques-testes.*** 2012. 126 f. Dissertação (Mestrado em Geotecnia) - Universidade Federal de Ouro Preto, Ouro Preto, 2012.

SAMPAIO, J. A.; ANDRADE, M. C.; DUTRA, A. J. B. ***Bauxita. Rochas e minerais industriais*****:** usos e especificações. CETEM. p. 279-304, 2005.

SANTOS, J. F.; SILVA, H. R.; PINTO, F. A.; ASSIS, I. R. D. Uso de imagens digitais para estimar a umidade do solo. ***Revista Brasileira de Engenharia Agrícola e Ambiental,*** v. 20, p. 1051-1056, 2016.

WANG, H. M.; SHI, P. Methods to extract images texture features. ***Journal of Communication University of China Science and Technology,*** p. 49-52, 2006.

Received: 4 March 2022 - Accepted: 29 May 2023.